American Journal of Pathology, Vol. 161, No. 5, November 2002

tau Assembly in Inducible Transfectants Expressing Wild-Type or FTDP-17 tau

Michael DeTure, Li-wen Ko, Colin Easson, and Shu-Hui Yen

From the Department of Neuroscience, Mayo Clinic Jacksonville, Jacksonville, Florida

Conditional expression systems for 4-repeat wild-type (WT) tau or the corresponding mutants V337M and R406W were established in human neuroglioma H4 cells to study the effect of tau mutations on the physicochemical properties of tau, and to develop a cellular model for the formation of filamentous tau characteristic of frontotemporal dementia with parkinsonism linked to chromosome 17 (FTDP-17) and Alzheimer's disease. Upon induction tau expression increased, reaching maximal levels at 5 to 7 days. WT tau was phosphorylated at amino acids T181, S202/T205, T231, and S396/S404. The R406W mutation decreased tau phosphorylation at each of these sites as did the V337M mutation except for S396/S404 sites that increased. Most tau in postnuclear cell lysates was recovered in the supernatant fraction after centrifugation at 200,000 × *g*. The amount of tau in the pellet fraction increased more in mutant transfectants compared to WT when the induction was extended beyond 5 days. This particulate tau could be partially extracted with salt, Triton X-100, or sarkosyl. Of the transfectants, R406W had the highest proportion of sarkosyl-insoluble tau by day 7. This insoluble fraction was thioflavin S-positive and contained 15- to 5-nm-wide filaments with tau immunoreactivities. The R406W filaments were more abundant than those detected in similar preparations from WT or V337M transfectants. At the light microscopy level, most tau was found with microtubules, or diffusely distributed in the cytoplasm, but none of this appeared thioflavin S-positive. The results suggest that conditional tau transfectants are in a pretangle stage making them an attractive model system for studying intracellular tangle accumulation and for testing potential therapeutic agents as inhibitors for tau aggregation. *(Am J Pathol 2002, 161:1711–1722)*

Filamentous tau inclusions represent a key pathological feature in Alzheimer's disease (AD) and FTDP-17 brains.[1,2] The role of these inclusions in neurodegeneration is not certain, but their abundance correlates positively with the severity of cognitive decline in AD patients.[3] This observation coupled with the discovery of tau mutations in FTDP-17 suggests that the accumulation of filamentous tau is detrimental to neuronal viability.[4–6] This view is supported by the creation of transgenic FTDP-17 animal models that exhibit neurofibrillary degeneration,[7,8] but the potential toxic effects of these tau accumulations and soluble tau still are not understood.[9,10]

FTDP-17 missense mutations, including V337M and R406W are located, respectively, within and flanking the microtubule (MT)-binding domain of tau that also constitutes the core of AD paired helical filaments.[11] The FTDP-17 mutations can inhibit tau-MT interactions *in vivo*[12] and/or promote tau self-assembly[13–15] and aggregation,[16] but the mechanism of FTDP-17 tau filament accumulation remains unclear. Phosphorylation of wild-type (WT) tau has been shown to modulate its binding to MTs and may lead to an increase in the pool of tau available for filament assembly in tauopathies. Hyperphosphorylated tau from AD brains not only has a decreased ability to promote MT polymerization, but it can strip normal tau from MTs. This causes MT depolymerization and leads to tau filament assembly.[17,18]

In vitro, GSK-3β has been shown to phosphorylate recombinant WT tau at the same sites as P301L and V337M mutants, but the R406W mutant was phosphorylated at only a subset of these sites.[19] Purification of WT and R406W tau from a FTDP-17 brain demonstrated a decrease in phosphorylation of the mutant tau in soluble cytosolic fractions, but not in sarkosyl-insoluble fractions.[20] In addition, studies on nonneuronal cells transfected with tau indicate that the expression of FTDP-17 tau affects cytoskeletal integrity differently than WT tau.[16,21–25] In these cell culture models, the transfected FTDP-17 tau appeared to be phosphorylated differently than WT tau, and mutants with increased aggregation did not bundle MTs as well as WT tau.[16] Filamentous tau inclusions were originally reported in a Δ280K CHO line, but the filaments were less than 10 nm in diameter; were not immunogold labeled; were not characterized for sarkosyl insolubility; and were not observed in WT, V337M, or R406W cell lines.[16] More recently, filamentous inclusions have been reported in okadaic acid/hydroxynon-

Supported by the National Institute on Aging (NIA) (grant AG AG17216 to S.-H. Y.) and the Mayo Foundation.

Accepted for publication July 25, 2002.

Address reprint requests to Shu-Hui Yen, Mayo Clinic Jacksonville, 4500 San Pablo Rd., Jacksonville, FL 32224. E-mail: yen.shu-hui@mayo.edu.

enal-treated SH-SY5Y neuroblastomas; but again these filaments were less than 10 nm in diameter and were poorly immunogold labeled with only one antibody to tau.[25] To date, none of the cell culture models have been shown convincingly to develop filamentous tau inclusions with structural, morphological, and biochemical properties consistent with those found in AD or related disorders, and this lack of filament formation in transient or most stable transfectants may indicate that cytosolic levels of tau are below the critical concentration. In this article, we describe the generation and characterization of conditional transfectants from human neuroglioma H4 cells expressing 4-repeat WT, V337M, or R406W tau. Using the tetracycline-off inducible mechanism to achieve more abundant tau expression, we examined the effects of FTDP-17 mutations on phosphorylation, aggregation, and filament assembly of tau. Glioma cells were used because abnormal accumulations of tau have been observed in glial cells,[26] and they have a relatively large cytoplasmic volume.

Materials and Methods

Antibodies

WKS44 was raised against a tau polypeptide corresponding to amino acid residues 162 to 178[27] and used at 1:250 dilution for immunofluorescence with the anti-tubulin TUB 2.1 (Sigma, St. Louis, MO) at 1:200 dilution. For immunofluorescence studies of tau phosphorylation, mouse monoclonal antibodies PHF1, CP13, TG3, AT180, and AT270, respectively, were used at 1:20, 1:75, 1:5, 1:75, and 1:75 dilution. PHF1, CP13, and TG3 were provided by Dr. P. Davies (Albert Einstein College of Medicine, Bronx, NY); AT180 and AT270 were purchased from Pierce Endogen (Rockford, IL). For Western blotting, tau antibodies were used at the following dilutions in the blocking solution: affinity-purified rabbit polyclonal WKS44 (1:1000), mouse monoclonals Tau46 (1:2000), PHF1 (1:100), CP13 (1:250), AT100 (1:250), AT180 (1: 250), AT270 (1:500), and TG3 (1:5). Tau46 recognizes tau peptides corresponding to amino acids 404 to 441. PHF1, CP13, AT100, AT180, TG3, and AT270 recognize sites phosphorylated, respectively, at S396/S404, S202/T205, T212/S214, T231, T231/S235, and T181. Other antibodies used for immunogold labeling were rabbit polyclonal E1 raised against a tau peptide corresponding to the tau sequence 19 to 33, mouse monoclonal anti-keratin, and anti-vimentin antibodies obtained from DAKO (Carpinteria, CA), and polyclonal antibodies to glial fibrillary acidic protein and neurofilament, respectively.[28]

H4 Neuroglioma Cells

A founder line, generated by transfecting human neuroglioma H4 cells with pUHD15-1neo (Clontech Laboratories Inc., Palo Alto, CA) that encodes tetracycline-repressible transactivator, was generously provided by Dr. R. E. Tanzi (Massachusetts General Hospital, Charlestown, MA). These cells, referred to as H4-15neo, were grown in Dulbecco's modified Eagle's medium (Life Technologies, Gaithersburg, MD) containing 10% fetal bovine serum (Life Technologies), 200 μg/ml G418 (Life Technologies), and 2 μg/ml tetracycline (Sigma) and maintained in a humidified incubator at 37°C with 5% CO_2.

Preparation of tau Plasmids for Transfection

The cDNA for 4-repeat WT (2-, 3-) tau in pBlueScript was provided by Dr. A. Andreadis (E. K. Shriver Center for Mental Retardation, Waltham, MA). They were digested with *Sal*I and cloned into the *Xho*I site of pcDNA3. The tau cDNAs from pcDNA3 were removed by digestion with *Eco*RI and then ligated into the tetracycline-responsive (pTRE) vector (Clontech, Palo Alto, CA).

To construct vectors containing tau with the V337M or R406W mutation, we used the site-directed mutagenesis strategy described before.[40] A reverse-strand oligo 5′-CCGCGAGACCCACCCTTGGAGGCTCCAGATTTATC-3′ was used with the following primers: V337M 5′-CAGGAG-GTGGCCAGATGGAAGTAAAATCTG-3′ or R406W 5′-GGGACACGTCTCCATGGCATCTCAGCAAT-3′ to mutate WT (2-, 3-) tau in pBlueScript using polymerase chain reaction with the aid of the Gene Editor Site-Directed Mutagenesis Kit (Promega, Madison, WI). The cDNAs were then cloned into pcDNA3 and pTRE. DH5α competent cells (Clontech) were transformed using the above pTRE constructs and plated to select positive clones. Colonies were picked, grown, and the pTRE plasmid containing the cDNA of interest was isolated using the Qiagen Maxi-Prep Plasmid Purification Kit (Qiagen, Santa Clarita, CA). The sequence and orientation were verified using an ABI377 automated sequencer with the Big Dye Terminator Sequencing Kit (Perkin Elmer, Norwalk, CT) and restriction enzyme size analysis, respectively.

Generation of Inducible tau Transfectants

The pTRE constructs from above and pBabe-Puro, a kind gift of Dr. T.-W. Kim (Massachusetts General Hospital, Boston, MA) were used to co-transfect H4-15neo founder cells with the aid of Tfx-20 (Promega). The cells were seeded in six-well plates at 4×10^5 cells per well. On the following day, cells were transferred to 100-mm dishes (Becton Dickinson Labware, Franklin Lakes, NJ) and selected with 1 μg/ml of puromycin (Sigma). Clonal cell lines were screened for inducible tau expression using the dual-immunofluorescence protocol described below.

Induction of tau Expression in Transfected H4 Cells

Transfected H4 cells were plated at 2 to 4×10^5 cells per dish (150-mm diameter, Becton Dickinson) in medium containing tetracycline. On the following day, the medium was removed and the cells were washed three times with 10 ml of Dulbecco's phosphate-buffered saline (PBS) (Life Technologies) before their incubation with medium lacking the tetracycline to induce tau expression. After

different durations of induction, cells were harvested to prepare lysates and insoluble tau fractions.

Double Immunofluorescence

Cells were plated on coverslips (5000 per well) in 24-well plates (Corning Inc., Corning, NY) and maintained as described above. At the end of induction, the coverslips were washed three times with 100 μl of stabilization buffer (80 mmol/L PIPES at pH 6.8, 1 mmol/L $MgCl_2$, 1 mmol/L EGTA, 1 mmol/L GTP, and 30% glycerol), dehydrated for 5 minutes in methanol, and fixed for 15 minutes in 2% paraformaldehyde made with stabilization buffer. The coverslips were then washed three times in 100 μl of stabilization buffer before the incubation with 10 mmol/L of phosphate at pH 6.8 and 137 mmol/L of NaCl (PBS) containing 0.3% Triton X-100 for 5 minutes to disrupt the cell membranes. After washing three times in 100 μl of 100 mmol/L Tris at pH 7.6 (TS), the coverslips were blocked for 30 minutes in TS containing 3% goat serum, followed by incubation for 30 minutes with a polyclonal anti-tau (WKS44) and a monoclonal anti-tubulin antibodies in TS containing 1% goat serum or WKS44 and a monoclonal antibody to phosphorylated tau epitope. The cells were washed six times with 100 μl of TS containing 1% goat serum and incubated for 30 minutes in the dark with fluorochrome-conjugated secondary antibodies (1/200), Alexa 594 goat anti-mouse IgG, and Alexa 488 goat anti-rabbit IgG (Molecular Probes, Eugene, OR), in TS containing 1% goat serum. The coverslips were washed and mounted on microscope slides using a 3:1 glycerol and PBS solution. The cells were viewed on a Leica Laborlux S microscope (Leica Microsystems, Wetzlar, Germany) with images collected using a 12-bit monochrome Minimax camera (Princeton Instruments Inc., Princeton, NJ). Data were collected and analyzed using the MCID software version 2.8 (Imaging Research Inc., St. Catherines, Ontario, Canada) to quantitate the relative phosphorylation of WT and mutant tau.

Preparation of Cell Lysates

After removal of feeding media and washing briefly with 10 ml of PBS, the cells were collected by scraping them off in 10 ml of PBS per 150-mm dish. The cells were counted, pelleted at 180 $\times$ *g* for 10 minutes, resuspended at 20,000 to 25,000 cells/μl in lysis buffer (20 mmol/L MES at pH 6.8, 80 mmol/L NaCl, 1 mmol/L $MgCl_2$, 2 mmol/L EGTA, 10 mmol/L NaH_2PO_4, 20 mmol/L NaF, 1 mmol/L phenylmethyl sulfonyl fluoride, and 10 μg/ml leupeptin) and then homogenized with 40 strokes using a Thomas pestle tissue grinder (Thomas Scientific, Swedesboro, NJ). The homogenates were centrifuged for 5 minutes at 500 $\times$ *g* to remove nuclei. The postnuclear lysates were collected and mixed 4:1 with 6$\times$ reducing sample buffer [375 mmol/L Tris, 12% sodium dodecyl sulfate (SDS), 12% β-mercaptoethanol, 60% glycerol, and 0.002% bromphenol blue at pH 6.8] giving a final concentration of 1.6 to 2.0 $\times$ 10^4 cells/μl of sample.

Preparation of Particulate tau

Postnuclear cell lysates prepared as described above were incubated at 4°C for 20 minutes to depolymerize MTs and then centrifuged for 20 minutes at 200,000 $\times$ *g*. Supernatants were collected and immediately mixed with 6$\times$ reducing sample buffer and boiled 10 minutes. The pellets were resuspended in a volume of lysis buffer equivalent to one fourth of the starting volume and immediately mixed with 6$\times$ sample buffer. This was done to adjust the amount of tau in the pellet samples so it more closely resembled that found in the supernatants. This facilitated the quantitation of the tau by densitometric analysis. Samples prepared from three to seven independent experiments were used for quantitative Western blotting analyses.

To determine the solubility of particulate tau from transfectants, the pellets were prepared in lysis buffer containing an additional 500 mmol/L NaCl, 1% Triton X-100, 1% Triton X-100 plus 0.5% deoxycholate plus 0.1% SDS or 500 mmol/L NaCl plus 10% sucrose plus 1% sarkosyl. The samples were vortexed for 30 minutes at room temperature and incubated another 30 minutes at 37°C (for those in NaCl or Triton X-100) or 4 hours at room temperature or overnight at 4°C (for those in sarkosyl) and centrifuged at 200,000 $\times$ *g* for 20 minutes. Again, supernatants were collected and mixed with 6$\times$ sample buffer. The pellets were resuspended with a Thomas pestle tissue grinder in a reduced amount of lysis buffer plus extracting agents. These pellet samples were then mixed with 6$\times$ sample buffer and analyzed by Western blotting. Sarkosyl-insoluble pellets were also resuspended as described and then mixed with 9 vol of 10 μmol/L of thioflavin S in 30 mmol/L of MOPs at pH 7.4 to assess filament formation.

Western Blot Analysis

Samples were run on 10% SDS-polyacrylamide gel electrophoresis gels and transferred to nitrocellulose paper overnight at 4°C. The blots were incubated with a blocking solution containing 5% milk proteins, 0.1% goat serum, and 0.1% Tween-20 in Tris-buffered saline (TBS) (25 mmol/L Tris, 150 mmol/L NaCl, pH 7.4) for 30 minutes before incubation with various tau antibodies for 1 hour at room temperature. The blots were washed three times with TBS containing 0.1% Tween-20, three times with TBS alone, and then incubated for 1 hour at room temperature with peroxidase-conjugated goat anti-rabbit or anti-mouse secondary antibodies (Chemicon, Temecula, CA) at 1:1000 dilution in blocking solution. After washing off the unbound antibodies, the blots were developed using enhanced chemiluminescence (Amersham Pharmacia Biotech, Uppsala, Sweden). To quantitate phosphorylation of total tau in lysates, blots were probed first with the rabbit polyclonal WKS44 and then reprobed with various mouse monoclonals (PHF1, CP13, AT180, AT270) to phosphorylated epitopes. Immunoreactivity of tau proteins was analyzed from scanned films using MCID software (Imaging Research Inc.), and the amount of phos-

phorylated epitope in each cell line was normalized to total tau for comparison of WT and mutant tau.

Thioflavin S Binding

Thioflavin S binding measured by fluorescence was used to determine the amount of tau filament formation in conditional transfectants using a Cary Eclipse fluorescence spectrophotometer (Walnut Creek, CA).[29] Sarkosyl-insoluble aggregates were collected as described and resuspended in 30 mmol/L of MOPs at pH 7.4 with 10 μmol/L of thioflavin S. These were then excited at 440 nm, and the emission spectrum was collected from 460 to 600 nm. The peak areas were integrated to get the fluorescence intensity. Noninduced transfectants were used as controls. Three separate experiments were performed, and the ratio of thioflavin S binding of induced/noninduced transfectant was determined by dividing the fluorescence intensity of sarkosyl-insoluble preparations from induced transfectants by the fluorescence intensity of identical preparations from noninduced transfectants.

Immunogold Electron Microscopy

Sarkosyl-insoluble samples, collected as described or fractionated further by sucrose gradient centrifugation, were examined by immunogold electron microscopy. The sucrose fractionation was performed by resuspension of the sarkosyl-insoluble samples in 1.5 ml of lysis buffer containing 10% (~0.3 mol/L) sucrose and running them on a step gradient containing 5 ml each of 1.5 mol/L and 2.0 mol/L sucrose in lysis buffer. After centrifugation at 160,000 $\times$ *g* for 16 hours, the following samples were collected: 2 ml at the top of the gradient, 4 ml of the 1.5 mol/L sucrose fraction, 1 ml at the 1.5/2.0 interface, 4 ml of the 2.0 mol/L sucrose, and 0.5 ml of the remaining 2.0 mol/L sucrose fraction including the pellet. The sarkosyl-insoluble materials were immediately adsorbed on to carbon/formvar-coated 400 mesh copper grids (EM Sciences) for 1 to 3 minutes or 15 to 60 seconds if unfractionated. The grids were washed three times with filtered TBS, blocked for 30 minutes on a filtered TBS solution containing 0.04% bovine serum albumin and 2% horse serum, and then incubated for 1 to 2 hours in primary antibody. Excess antibodies were removed by washing three times in blocking solution, and the grids were incubated for 1 hour in solutions containing Aurugold 5-nm gold-conjugated anti-rabbit or 10-nm gold-conjugated anti-mouse secondary antibody (1:20 dilution, Amersham). After washing five times with TBS, the grids were stained with 2% uranyl acetate for 45 seconds and examined with an EM 208S electron microscope (Phillips, Hillsboro, OR). All antibodies were diluted with the blocking reagent. The tau primary antibodies used were the mouse monoclonal Tau46 (1:50) and the rabbit polyclonal E1 (1:20). Samples incubated without primary antibodies or with mouse monoclonal antibodies to tubulin (1:15), keratin (1:100), and vimentin (1:100) were used as negative controls. Electron micrographs containing filaments with at least four gold particles were scanned, and length measurements were taken using the MCID software.

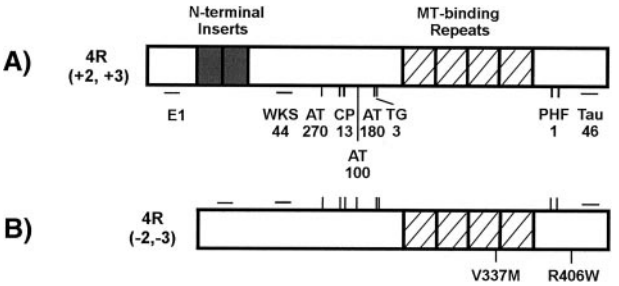

Figure 1. Schematic representation of human brain tau. **A:** Full-length 4-repeat tau with 441 amino acid residues [4R (+2, +3)]. **B:** Full-length 4-repeat tau with 383 amino acid residues lacking exons 2 and 3 [4R (−2, −3)]. The sites of the N-terminal inserts, MT-binding repeats, mutations, and epitopes recognized by antibodies to nonphosphorylated tau (WKS44, E1, and Tau46) and phosphorylated tau (AT270, CP-13, AT-100, AT-180, TG-3, and PHF-1) are marked.

Results

Immunolabeling of Cell Lines for tau Expression

Cells transfected with WT or FTDP-17 (2-, 3-) tau cDNA in the inducible pTRE vector (Figure 1) were screened for tau expression after 3 days of induction. Transfectants maintained in media containing tetracycline were used as controls. The screening was accomplished by monitoring tau expression in fixed H4 cells grown on glass coverslips. WKS44, which recognizes total tau, was used in conjunction with a mouse monoclonal anti-tubulin antibody (TUB2.1) to determine whether the tau was colocalized with the MT network. Cell lines that expressed the highest levels of tau after 3 days of induction and contained undetectable amounts of tau without the induction were chosen for further characterization. In these transfectants, tau immunoreactivities were detected with MT networks and MT bundles (Figure 2). They also distributed diffusely in the cytoplasm. The bundling was observed more frequently in WT and R406W transfectants than in the V337M line (Figure 2) and was never detected in the pTRE vector control line lacking tau cDNA (data not shown). Together this indicates that most V337M cells did not express the highest levels of tau. The expression of tau in each of the transfectants with a 5-day or shorter induction was not uniform, and cells expressing higher levels of tau often were observed next to cells producing little or no tau (Figure 2). After 7 days of induction, most cells in each line displayed some tau immunoreactivities. In contrast to other transfectants, most of the V337M cells expressed comparable levels of tau, whereas WT or R406W tau expression varied widely in cells belonging to the same transfectant.

Immunoblotting of Lysates from tau Transfectants

Western blotting of postnuclear cell lysates from WT and mutant transfectants was used to verify tau expression on induction. In the presence of tetracycline, tau was not

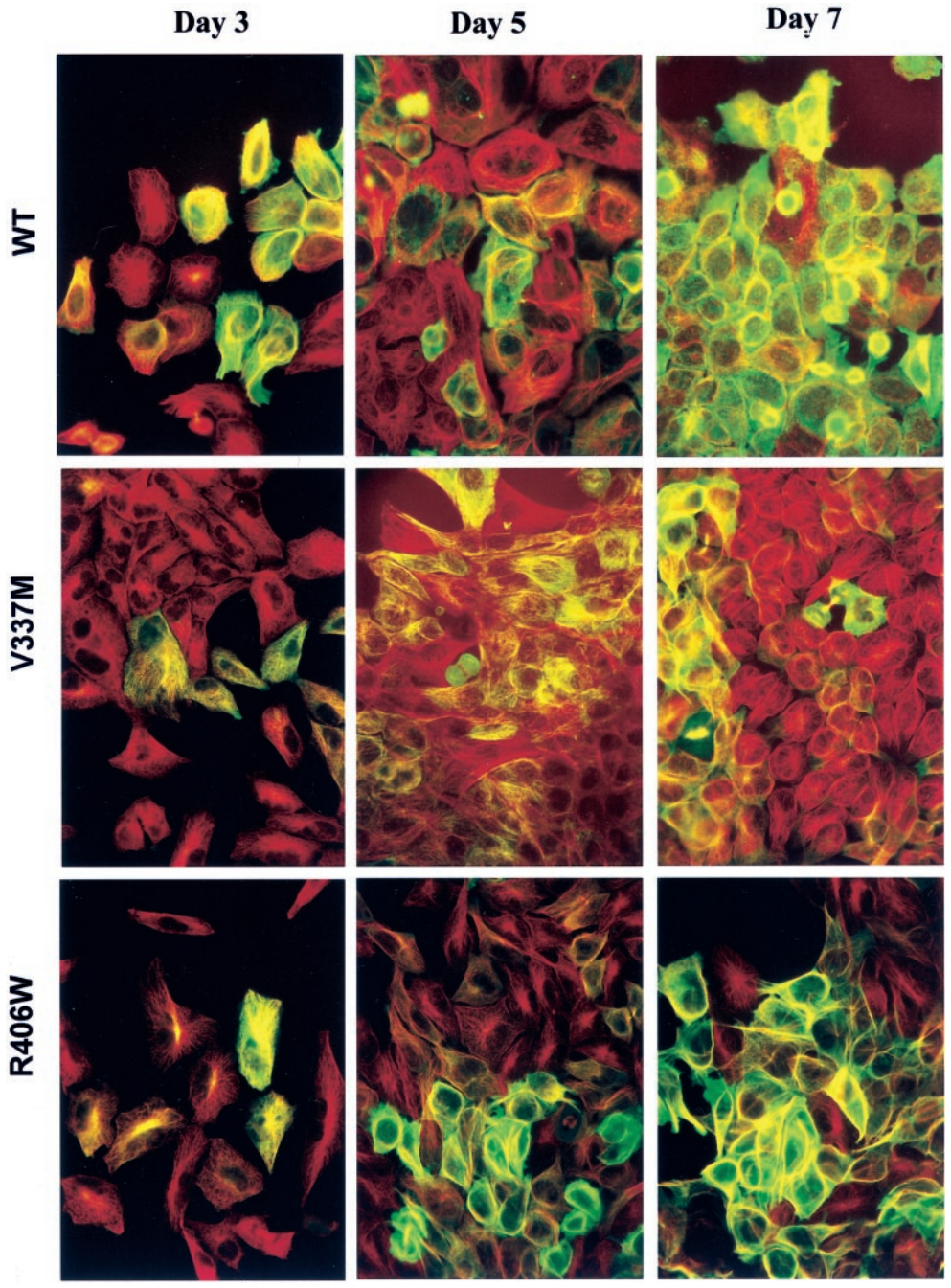

Figure 2. Double-immunofluorescence staining of tau transfectants. Cells were labeled with antibodies to tau (green) and tubulin (red). Transfectants expressed variable levels of tau after 3 days of induction, but by 7 days of induction most of the cells expressed tau. As the expression of tau increased the MT network becomes reorganized. Co-localization of tau and MT (orange to yellow color) was observed in cells expressing low levels of tau; but as levels of tau increased, tau was observed in MT bundles and in regions of cytosol lacking of MTs. By day 7, most of the cells have tau expression.

detectable by Western blotting (Figure 3A, day 0). In comparison, tau was detected within 24 hours of tetracycline removal. The level of tau appeared to reach its maximum by day 7 (Figure 3A). Extension of the induction period beyond 5 to 7 days led to generation of small amounts of degraded tau fragments that were smaller in molecular weight than 4-repeat recombinant tau.

The level of tau in lysates from different transfectants was determined by using different known amounts of recombinant WT tau as standards in immunoblotting. Densitometric analyses of Western blots of lysates from comparable number of cells with a 5-day induction demonstrated that the WT sample contained ~40% more tau than either V337M or R406W. With a 7-day induction, the amount of tau detected in WT, V337M, and R406W, respectively, were 12.6 ± 3.8 (average ± SEM), 6.8 ± 2.0, and 5.1 ± 2.8 μg per 10^6 cells, and these levels were often approached after only 5 days of induction. At these levels, tau saturated the MT network generating large amounts of free cytosolic tau.[30]

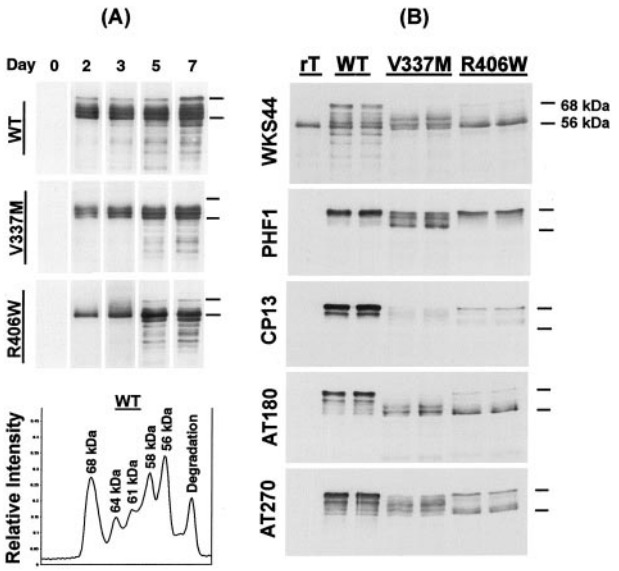

Figure 3. Western blotting of postnuclear lysate from inducible transfectants. **A:** Time-dependent induction of tau expression: lysates obtained 0, 2, 3, 5, and 7 days after tetracycline-off induction were subjected to Western blotting using WKS44, an antibody to nonphosphorylated tau epitopes. Recombinant 4R (−2, −3) tau (rT) and molecular weight standards (not shown) were used as references. The lysates from WT transfectants contain tau species of 68, 64, 61, 58, 56 kd, and lower molecular weight. tau species larger than the recombinant standard (56 kd) in size are regarded as intact tau with post-translational modifications. **B:** Phosphorylation of lysates from transfectants with a 5-day induced expression of WT (**lanes 2** and **3**), VM (**lanes 4** and **5**), and RW tau (**lanes 6** and **7**) were probed with WKS44, PHF1, CP13, AT180, and AT270. Four-repeat (2-, 3-) recombinant tau was included as a reference. The location of 68-kd and 56-kd regions are marked. All samples displayed phosphorylated tau immunoreactivities. However, the labeling pattern and the relative levels of different phospho-tau species were different between the WT and mutant tau (Table 1).

The WT and mutant tau differed in their electrophoretic profiles. When lysates from WT transfectant were probed with tau antibodies to nonphosphorylated epitopes with WKS44 five bands of molecular weight equal to or higher than that of recombinant tau (56 kd) were detected (Figure 3A). Densitometric scanning of immunoblots showed that the largest tau species in the WT transfectants was 68 kd in molecular weight and was in low abundance or absent in the corresponding V337M and R406W transfectants. tau of 64, 61, 58, and 56 kd were also detected in the WT transfectants. Of the four tau species, the 64-kd band was not readily detected in the lysates from V337M and R406W transfectants and the 61- and 58-kd tau were missing or in low abundance in R406W but not V337M tau. The 56-kd band was the most abundant species for R406W giving it the simplest profile. Such differences between mutant and WT tau in gel electrophoretic profiles were observed in transfectants with different durations of tau expression and expression levels.

Analyses of tau Phosphorylation

The differences in electrophoretic mobility observed among WT, V337M, and R406W tau are likely because of changes in phosphorylation. This is supported by the data obtained from immunoblotting of cell lysates with a series of antibodies specific to different phosphorylated tau epitopes (Figure 3B). In WT tau, both the 68-kd and 64-kd bands displayed CP13, AT180, and AT270 immunoreactivities, and only the 68-kd tau was labeled by PHF-1. In comparison, smaller intact tau displayed very little phospho-tau immunoreactivities except with AT180. Phosphorylated tau epitopes were also detected in V337M and R406W tau, but the patterns and the intensities of immunolabeling were different from that displayed by WT tau. In addition to the aforementioned antibodies, lysates were also probed with two other phosphorylation-sensitive tau antibodies, TG3 and AT100, but weak immunoreactivity was only detected after 9 to 15 days of induction.

To compare the extent of phosphorylation in mutant and WT tau, lysates obtained from transfectants with a 5-day induction were probed with WKS44 and double-labeled with PHF1, CP13, AT180, and AT270, respectively. The volumes of lysates loaded for Western blots were adjusted so the WKS44 immunoreactivities of undergraded tau for each transfectant were comparable and the major bands are within the linear range of recombinant tau standards. The area of tau bands marked for quantitation of WKS44 immunoreactivities was identical to that marked for quantitation of phospho-tau immunoreactivities. This allowed for more consistent densitometric quantitation of the phosphorylated and nonphosphorylated tau. Comparison of the ratio between phosphorylated and nonphosphorylated tau immunoreactivities of intact tau in different lysates revealed differences between WT and mutant tau in the extent of phosphorylation (Table 1). Statistical analysis of four separate preparations demonstrated that R406W tau was significantly ($P < 0.02$) less phosphorylated than WT tau at PHF1, CP13, AT180, and AT270 epitopes. Similarly, V337M was less phosphorylated than WT at all epitopes examined ($P < 0.02$) except the PHF1 site, which was more phosphorylated than WT tau ($P < 0.02$).

To verify the Western blotting findings, transfectants with a 5-day induction were double-labeled with WKS44 and PHF1, CP13, AT180, or AT270 (Figure 4), and the intensity of fluorescence signal from each cell (or a small

Table 1. Relative Phosphorylation of WT and Mutant tau at the PHF1, CP13, AT180, and AT 270 Sites Assessed by Western Blotting

Tau isoform	PHF1/WKS44	CP13/WKS44	AT180/WKS44	AT270/WKS44
WT	1.00 (0.09)	1.00 (0.09)	1.00 (0.17)	1.00 (0.16)
V337M	1.41 (0.29)	0.15 (0.04)	0.72 (0.15)	0.45 (0.17)
R406W	0.76 (0.14)	0.17 (0.03)	0.74 (0.18)	0.33 (0.07)

Note: The mutant values are statistically different from the WT ($P < 0.02$, $n = 4$). The numbers shown in parentheses represent standard deviations.

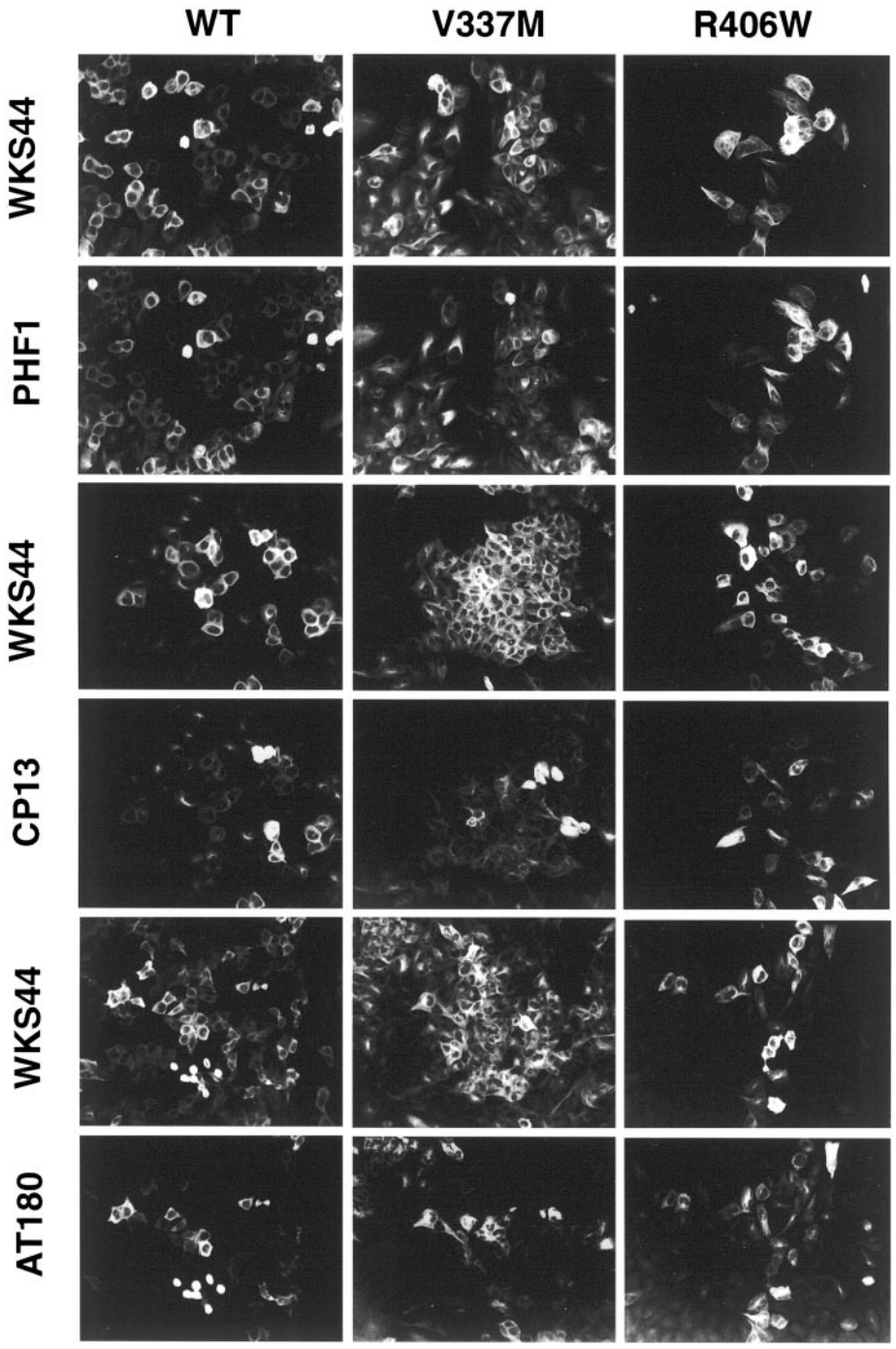

Figure 4. Immunofluorescence staining of phosphorylated tau in inducible transfectants. WT, V337M, and R406W transfectants after a 5-day induction were labeled with WKS44 (recognizes nonphosphorylated tau) and PHF1, CP13, or AT180 (recognizes phosphorylated tau). Many cells were intensely labeled with WKS44, but immunoreactivity with PHF1, CP13, or AT180 antibodies to phosphorylated epitopes varied greatly (Table 2). Some of these images were adjusted to view the CP13 and AT180 better.

group of cells with similar immunoreactivity) was quantitated by image analysis. Cells containing similar levels of tau (based on WKS44 fluorescence immunoreactivity) were compared for their CP13, AT180, and PHF1 immunoreactivities. Three hundred to six hundred cells from each transfectant were analyzed, and the analysis was repeated with duplicated samples. The results (Table 2) are in agreement with those derived from Western blot analyses of total cell lysates by demonstrating an increase of PHF1 staining in V337M and a decrease of PHF1 phosphorylation in R406W when compared to WT tau. Likewise, the CP13 and AT180 immunoreactivities were both decreased in the V337M and R406W tau when compared to WT. Immunofluorescent quantitation was not done with AT270 as the antibody stained some nuclear antigens not recognize by all other tau

Table 2. Relative Phosphorylation of WT and Mutant tau at the PHF1, CP13, and AT180 Assessed by Immunofluorescence

Tau isoform	PHF1/WKS44	CP13/WKS44	AT180/WKS44
WT	1.00 (0.10)	1.00 (0.08)	1.00 (0.05)
V337M	1.27 (0.03)	0.50 (0.09)	0.32 (0.06)
R406W	0.71 (0.09)	0.72 (0.07)	0.47 (0.07)

Note: The mutant values are statistically different from the WT ($P < 0.001$, $n = 300$ to 600). The results were unchanged when excluding mitotic cells or those cells with lower tau expression. The numbers shown in parentheses represent standard deviations.

antibodies tested. The data demonstrate clearly that V337M and R406W mutations alter tau phosphorylation at sites distant from the mutations.

Particulate tau

To determine whether expression of mutant tau leads to generation of tau aggregates similar to those observed with FTDP-17 brain tissue preparations, lysates were prepared from transfectants with increasing induction periods under MT depolymerizing conditions and centrifuged at high speed to obtain a particulate tau fraction (Figure 5). The amounts of tau present in the supernatant and corresponding pellet were determined by densitometric analysis of immunoblots, and the proportion of tau distributed in the pellet and lysate was calculated. Such analyses demonstrated that after 3 days of induction 10% of the tau in all transfectants was pelletable. There were no significant differences between the WT and mutants samples in the proportion of particulate tau unless the induction time was extended. By 7 days of tau induction, 13 ± 3% (average ± SD) and 17 ± 2%, respectively, of the V337M and R406W tau were recovered in the pellet fraction. In contrast, the proportion of WT tau in the pellet fraction (10 ± 3%) was not changed even though WT transfectants expressed the most tau. These increases in the amount of particulate tau in V337M and R406W cell lines at day 7 were significant compared to WT ($P < 0.05$, $P < 0.005$; $n = 7$).

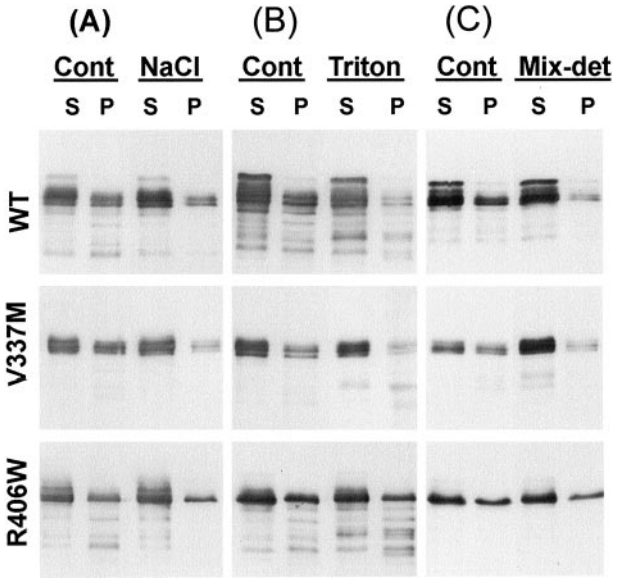

Figure 5. Western blotting of fractionated lysates with WKS44. Lysates were extracted from transfectants with 7 days of induction under MT depolymerizing conditions. The extraction was performed with lysis buffer alone (Cont), supplemented with 500 mmol/L NaCl (**A**), 1% Triton X-100 (**B**), or 1% Triton X-100 plus 0.1% SDS and 0.5% deoxycholate (Mix-Det) (**C**). Supernatant (S) and pellet (P) fractions were separated by high-speed centrifugation. All pellets were dissolved in sample buffer in a volume equivalent to one fourth of that of the lysates. Analyses of multiple blots from six separate preparations demonstrated that mutant transfectants contain a higher proportion of tau in the pellet fraction than WT. Multiple blots from three separate preparations were analyzed. tau in R406W transfectants were the least susceptible to each extraction followed by WT and V337M.

Three batches of transfectants after 7 days of induction were further examined to determine the solubility properties of particulate tau. In the presence of 500 mmol/L of NaCl (Figure 5A) or 1% Triton X-100 plus 0.5% deoxycholate and 0.1% SDS (Figure 5C), more than 90 ± 10% of the particulate V337M could be solubilized. In contrast, only 65 ± 14% and 55 ± 2%, respectively, of the particulate tau in WT and R406W were solubilized by the same reagents, suggesting that some of the particulate tau are peripherally associated with membranes. It is not clear why V337M tau is more soluble in these detergents than other forms of tau. Perhaps, the region of tau involved in association with membranes is affected by the V337M mutation because of an alteration of tau's conformation. Transfectants with 7 or more days of induction were further demonstrated to contain tau resistant to 500 mmol/L NaCl, 0.3 mol/L sucrose, and 1% sarkosyl (Figure 6A). This form of tau was estimated to account for 0.5 ± 0.2% of total tau in R406W and less than 0.1% in WT or V337M. The results demonstrate that, similar to AD brains and FTDP-17 transgenic mice, conditional transfectants contain sarkosyl-insoluble tau.

Sarkosyl-insoluble fractions from AD contain tau-paired helical filaments capable of binding thioflavin S.[31] This fluorescence assay was used to assess whether sarkosyl-insoluble fractions from H4 cells contained tau aggregates similar to those in AD. The results (Figure 6B) clearly showed that there were differences between induced and noninduced (NI) transfectants in thioflavin S binding. After 7 days of induction, the R406W transfectants (2.1 ± 0.2 × NI) generated more sarkosyl-insoluble, polymerized tau, than WT (1.7 ± 0.1 × NI) or V337M (1.7 ± 0.3 × NI) transfectants. The difference between R406W was statistically significant ($P < 0.02$, $n = 3$). With 5 days of induction, only sarkosyl-insoluble preparations from R406W transfectant displayed thioflavin S binding higher (1.2 × NI) than that measured in noninduced transfectants.

The possibility that the pelletable tau fractions resistant to membrane-solubilizing agents might have contained filamentous tau was explored further with immunogold electron microscopic analysis of cell lysates insoluble in sarkosyl and fractionated by resuspension in 0.3 mol/L of

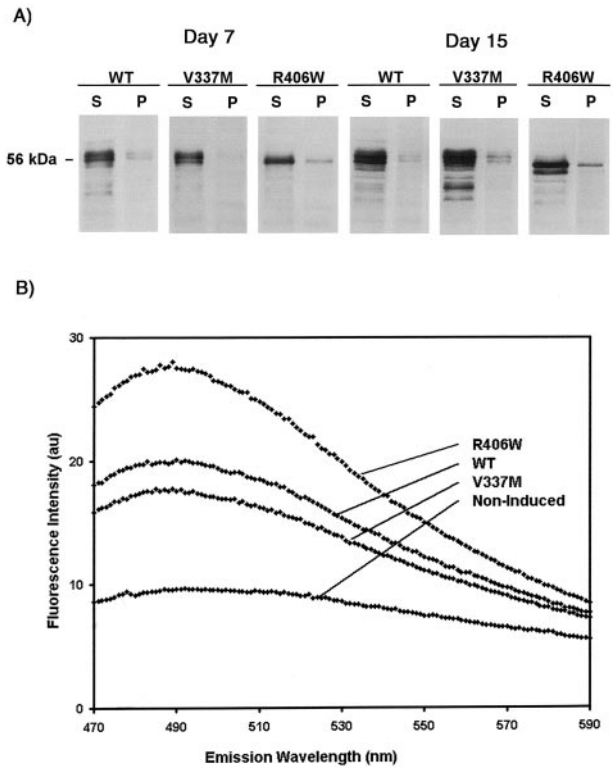

Figure 6. A: Western blotting of samples obtained from extraction of the pellets derived from Figure 5 (Cont, P) with lysis buffer supplemented with 500 mmol/L of NaCl, 10% sucrose, and 1% sarkosyl. The sarkosyl-soluble (S) and -insoluble pellet (P) fractions were separated by centrifugation at high speed. The pellets were resuspended in sample buffer at a volume equivalent to one half the volume of the extracts. Sarkosyl-insoluble tau was detected in transfectants after 7 days of induction. Such insoluble tau were more abundant in R406W transfectants and were also detected in cells replated after 8 days of induction and maintained for another 7 days in the absence of tetracycline. **B:** Thioflavin S binding to sarkosyl-insoluble preparations of H4 transfectants. To control for background fluorescence in noninduced (NI) transfectants, fluorescence intensities were normalized to NI signals. Experiments were repeated in triplicate. WT preparations had thioflavin S signals of 1.7 ± 0.1 × NI signals whereas V337M and R406W were 1.7 ± 0.3 × NI and 2.1 ± 0.2 × NI, respectively. The increase in R406W compared to WT was found to be significant ($P < 0.02$).

sucrose and separation on a sucrose step gradient containing 1.5 mol/L and 2.0 mol/L of sucrose cushions. Similar sarkosyl-insoluble preparations from AD or FTDP-17 brains have previously been shown to contain tau proteins with filamentous structures.[1,31] Samples were collected from each sucrose step and the interfaces between steps and then subjected to immunogold electron microscopy with antibodies to the amino (E1)- and/or carboxy-terminus (Tau46) of tau. Filamentous structures of 15 to 25 nm in diameter were decorated with immunogold (Figure 7; A to D), and very few gold particles were detected in nonfilamentous elements. Both E1 and Tau46 immunoreactivities were detected in these filaments (Figure 7D, inset). Unlike paired helical filaments observed in AD, the filaments made by transfectants did not exhibit regular twisting. Most of the tau filaments derived from cultured cells after 7 days of induction were less than 500 nm in length (Figure 7C), but occasionally longer filaments were found (Figure 7D). tau filaments were more readily detected in samples collected at the interface between the 1.5-mol/L and 2.0-mol/L sucrose steps, and filaments were more abundant in R406W (Figure 7, C and D) samples than WT and V337M transfectants (Figure 7, A and B). Moreover, the average filament length for R406W (339 ± 152 nm) was greater ($P < 0.02$) than that observed from WT (168 ± 44 nm) or V337M (172 ± 28 nm) transfectants. This confirms the thioflavin S-binding data that there was more total assembled tau from R406W transfectants than WT or V337M preparations. Very few tau filaments were detected in R406W with 5 days of induction even though the level of tau was ~90% of that with 7 days of induction. The results suggest that the polymerization of tau is time-dependent. No tau filaments were observed in WT and V337M samples with 0 to 5 days of induction or in R406W samples with 0 to 3 days of induction. Immunogold double labeling of duplicated samples with polyclonal antibodies to tau and monoclonal antibody to tubulin, vimentin, or keratin did not detect the staining of tau filaments with antibodies to non-tau proteins; and similarly Western blotting of sakosyl-insoluble samples from WT, V337M, or R406W transfectants were negative for neurofilament or glial fibrillary acidic proteins (data not shown).

It is unlikely that tau filaments observed in sarkosyl-insoluble preparations were formed after cell lysis, because the lysates were kept at 4°C or processed immediately. In fact, storage of samples at 4°C overnight did not lead to a noticeable increase of tau filaments while storage for increasing periods at 4°C reduced the amount of gold-labeled tau filaments observed (data not shown). Moreover, addition of recombinant tau to lysates from vector control transfectants did not lead to the generation of tau filaments, and these same lysates interfered with heparin-promoted assembly of recombinant tau in a dose-dependent manner (data not shown). Staining of fixed cells with thioflavin S did not label any structures resembling neurofibrillary tangles, and tau-transfected cells displayed only occasional weak, homogenous staining at intensities less than twice background levels (data not shown). The detection of significant thioflavin S binding and fluorescence in sarkosyl-insoluble fractions but not fixed cells likely resulted from increasing the tau filament concentration during fractionation and pelleting. Together, the data demonstrate that tau transfectants are capable of producing tau filaments and that these cells resemble pretangles containing neurons in their absence of thioflavin S staining in a fibrous pattern.

Discussion

Excessive amounts of WT or mutant tau may be toxic to cells and prevent the cloning of stable transfectants with high levels of tau expression. To circumvent this problem, the tetracycline-off inducible system was used in the present studies to generate high concentrations of cytosolic tau in cultured cells and to develop a cellular model for tau filament formation. Moreover, analyses of H4 cell lysates from induced transfectants clearly demonstrated that mutant and WT tau had different biochemical and physicochemical properties. The gel electrophoretic analyses showed R406W tau from H4 cells migrated

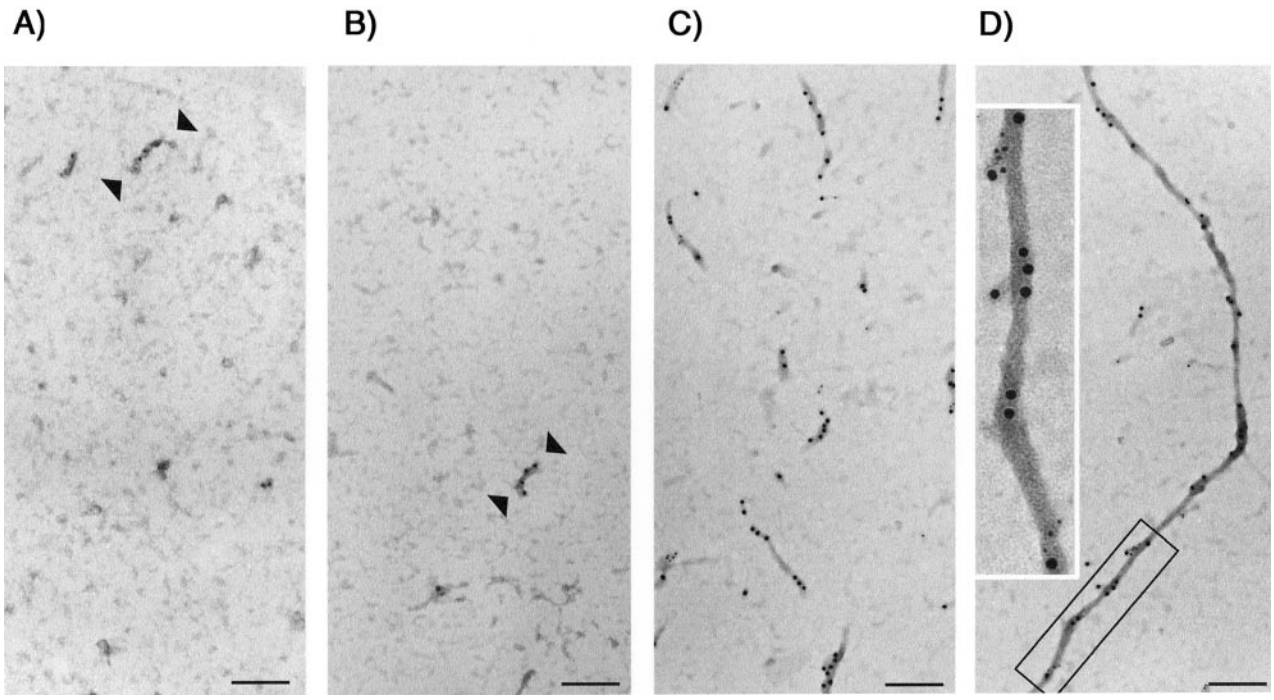

Figure 7. Immunogold labeling of sarkosyl-insoluble preparations enriched with filaments. Sarkosyl-insoluble samples were separated on a sucrose step gradient. Samples collected from the 1.5 mol/L/2.0 mol/L interface were adsorbed onto electron microscopy grids and immunogold labeled with Tau46, a mouse monoclonal against the carboxy-terminus of tau (10-nm gold) and E1, a rabbit polyclonal antibody to the amino-terminus of tau (5-nm gold). More filaments were detected in R406W (**C–D**) than WT (**A**) or V337M (**B**) samples. These filaments are not uniform in diameter and do not display morphology characteristic of paired helical filaments. Scale bar, 195 nm. The **inset** in **D** displays the boxed tau filament with an additional ×2.2 of magnification.

mostly as one band of 56 kd. This pattern is similar to that reported for the same form of tau expressed in stable CHO transfectants,[16] and the 4-repeat (2+, 3+) R406W tau isoform[22] transiently expressed in COS cells. The gel electrophoretic profile of WT and V337M tau from H4 cells did however differ from the same tau isoforms expressed by transiently transfected CHO and COS cells reported earlier.[24,32] Because S202/T205 (CP13/AT8 epitope) is phosphorylated in WT transfectant derived from H4, but not CHO cells, the discrepancy could be because of differences in kinases/phosphatases between human and nonhuman cells or central nervous system and non-central nervous system cells. Alternatively, tau in transient transfectants may not have sufficient time to achieve the same extent of phosphorylation as those in stable transfectants. This possibility, however, is not supported by our observation of the phosphorylation of S202/T205 or S396/S404 in H4 transfectants after 1 day of induction.

tau proteins are substrates of a number of kinases, and they are phosphorylated at multiple sites. A decrease in S396/S404 phosphorylation has previously been reported in CHO and COS cells transiently transfected with R406W mutant tau.[22,24,33] Our results indicate that FTDP-17 mutations alter the susceptibility of tau to phosphorylation at multiple sites, and this was not limited to serine or threonine residues near the mutation, raising the possibility that FTDP-17 mutations may change the conformation of tau in regions as far as 200 amino acid residues from the site of mutation. It is possible these mutations cause conformational changes that mimic AD pathogenic phosphorylation or alter the accessibility of tau to certain kinases and phosphatases. This view is consistent with that reported in a recent study[19] and is also supported by the finding of differences between recombinant mutant and WT tau in circular dichroism spectra.[34] On the other hand, similar biophysical analysis performed by others has failed to generate comparable results.[35] Two studies have shown that close association between the amino terminus and the middle region of tau molecule is necessary for the generation of the Alz50 epitope specific for AD abnormal pathological tau.[36,37] Similar conformational changes may be achieved in AD by hyperphosphorylation and in FTDP-17 by missense mutations.

H4 cells expressing mutant or WT tau are heterogeneous in morphology, reflecting different degrees of tau induction in an asynchronous culture. The immunofluorescence data could not distinguish any differences in MT binding between the WT and mutant tau, suggesting that V337M and R406W mutations may not have a major impact on tau-MT interactions. There may be differences between WT and mutants in binding affinity for the MTs,[38–40] but as the high levels of tau in H4 cells saturate the endogenous MTs, studies of relative MT affinity were not undertaken. Small differences between mutant and WT tau in their affinity for MT binding could precipitate tau inclusion formation in neurons containing both forms of tau. This is supported by a recent study that showed expression of only WT or mutant tau led to similar MT binding behavior in transfected cells, but co-expression of WT and mutant tau led to the distribution of mutant tau diffusely in the cytoplasm, whereas WT associated with

MTs.[41] Free mutant tau might polymerize into filaments if the critical concentration were reached. This is consistent with our present findings of sarkosyl-insoluble tau filaments in conditional transfectants that contain high levels of tau.

tau aggregates have previously been detected immunocytochemically in stable CHO transfectants expressing Δ280K mutation or tau with three FTDP17 mutations.[16] These aggregates contain filaments of diameter that are equal to or smaller than 10 nm, which differs from the tau filaments formed in conditional tau transfectants. Because the sarkosyl solubility of tau aggregates generated in CHO cells was not reported, it remains uncertain whether they are comparable to tau aggregates developed in various tauopathies. Another distinction between H4 and CHO transfectants is that CHO cells expressing WT, V337M, or R406W tau did not produce tau aggregates. This likely results from the increased tau expression that was achieved by using the inducible mechanism, but it may also reflect intrinsic differences between the CHO cells and human H4 neurogliomas in the ability to form tau aggregates. Based on our immunoblotting and thioflavin-binding assays, it was apparent that less sarkosyl-insoluble aggregated tau formed in WT and V337M transfectants than in R406W transfectants with 7 days of induction. The relative extent of tau aggregation detected between different transfectants by three methods is not the same. Perhaps this is because of the exclusion of measuring smaller tau aggregates in immunoelectron microscopic analyses. The results, however, do not necessary indicate that the assembly of V337M tau is slower than R406W, because cells in the V337M line are more uniform in tau expressions than WT or R406W cell lines. It is possible that the lower production of sarkosyl-insoluble tau in V337M is because of the absence of cells with a high concentration of tau relative to WT or R406W.

Immunogold electron microscopy and thioflavin S-binding studies revealed that the decrease of tau solubility in sarkosyl was associated with the formation of tau filaments. Filament formation probably reflects the fact that transfectants have tau that reached the concentration critical for self-assembly, but it might also result from the abnormal expression or distribution of molecules capable of promoting tau assembly as a cellular response to the presence of excess cytoplasmic tau. tau filaments produced by H4 cells were not detectable at the light microscopic level by thioflavin S staining, and tangle-like staining was not observed using immunofluorescence and a variety of antibodies to tau. The question remains why transfectants were able to generate tau filaments, but failed to develop tangle pathology. One possibility is that the formation of tangles requires a longer period of interactions between tau filaments or a higher concentration of filaments, and such durations and levels were not reached in 7- to 15-sday transfectants. Additionally, the presence of additional factors may be needed for the bundling of tau filaments into tangles, and these may only be produced during aging or under oxidant stress. In summary, a cellular model of tau aggregation with pretangle formation and filament assembly has been generated. The model will be explored for usage in studying the mechanism of intracellular tangle formation, identifying stresses that might facilitate tangle formation during aging or AD, and in testing the ability of potential therapeutic agents in inhibiting tau assembly.

Acknowledgments

We thank Dr. Wen-Lang Lin for his assistance in electron microscopy, and Drs. Dennis W. Dickson and Naruhiko Sahara for their comments on the manuscript.

References

1. Spillantini MG, Van Swieten JC, Goedert M: Tau gene mutations in frontotemporal dementia and parkinsonism linked to chromosome 17 (FTDP-17). Neurogenetics 2000, 2:193–205
2. Heutink P: Untangling tau-related dementia. Hum Mol Genet 2000, 9:979–986
3. Nagy Z, Esiri MM, Jobst KA, Morris JH, King EM, McDonald B, Litchfield S, Smith A, Barnetson L, Smith AD: Relative roles of plaques and tangles in the dementia of Alzheimer's disease: correlations using three sets of neuropathological criteria. Dementia 1995, 6:21–31
4. Hutton M, Lendon CL, Rizzu P, Baker M, Froelich S, Houlden H, Pickering-Brown S, Chakraverty S, Isaacs A, Grover A, Hacket J, Adamson J, Lincoln S, Dickson D, Davies P, Petersen RC, Stevens M, de Graaf E, Wauters E, van Baren J, Hillebrand M, Joosse M, Kwon JM, Nowotny P, Kuei Che L, Norton J, Morris JC, Reed LA, Trojanowski J, Basun H, Lannfelt L, Neystat M, Fahn S, Dark F, Tannenberg T, Dodd P, Hayward N, Kwok BJ, Schofield P, Andreadis A, Snowden J, Craufurd D, Neary D, Owen, Oostr B, Hardy J, Goate A, Van Swieten J, Mann D, Lynch T, Heutink P: Association of missense and 5′-splice-site mutations in tau with the inherited dementia FTDP-17. Nature 1998, 393:702–705
5. Poorkaj P, Bird TD, Wijsman E, Nemens E, Garruto RM, Anderson L, Andreadis A, Wiederholt WC, Raskind M, Schellenberg GD: Tau is a candidate gene for chromosome 17 frontotemporal dementia. Ann Neurol 1998, 43:815–825
6. Spillantini MG, Murrell JR, Goedert M, Farlow MR, Klug A, Ghetti B: Mutation in the tau gene in familial multiple system tauopathy with presenile dementia. Proc Natl Acad Sci USA 1998, 95:7737–7741
7. Lewis J, McGowan E, Rockwood J, Melrose H, Nacharaju P, Van Slegtenhorst M, Gwinn-Hardy K, Murphy M, Baker M, Yu X, Duff K, Hardy J, Corral A, Lin WL, Yen SH, Dickson DW, Davies P, Hutton M: Neurofibrillary tangles, amyotrophy and progressive motor disturbance in mice expressing mutant (P301L) tau protein. Nat Genet 2000, 25:402–405
8. Gotz J, Chen F, Barmettler R, Nitsch RM: Tau filament formation in transgenic mice expressing P301L tau. J Biol Chem 2000, 276:529–534
9. Furukawa K, D'Souza I, Crudder CH, Onodera H, Itoyama Y, Poorkaj P, Bird TD, Schellenberg GD: Pro-apoptotic effects of tau mutations in chromosome 17 frontotemporal dementia and parkinsonism. Neuroreport 1999, 11:57–60
10. Wittmann CW, Wszolek MF, Shulman JM, Salvaterra PM, Lewis J, Hutton M, Feany MB: Tauopathy in Drosophila: neurodegeneration without neurofibrillary tangles. Science 2001, 293:711–714
11. Wischik CM, Novak M, Thogersen HC, Edwards PC, Runswick MJ, Jakes R, Walker JE, Milstein C, Roth M, Klug A: Isolation of a fragment of tau derived from the core of the paired helical filament of Alzheimer disease. Proc Natl Acad Sci USA 1988, 85:4506–4510
12. Nagiec EW, Sampson KE, Abraham I: Mutated tau binds less avidly to microtubules than wildtype tau in living cells. J Neurosci Res 2001, 63:268–275
13. Nacharaju P, Lewis J, Easson C, Yen S, Hackett J, Hutton M, Yen SH: Accelerated filament formation from tau protein with specific FTDP-17 missense mutations. FEBS Lett 1999, 447:195–199
14. Goedert M, Jakes R, Crowther RA: Effects of frontotemporal dementia

FTDP-17 mutations on heparin-induced assembly of tau filaments. FEBS Lett 1999, 450:306–311
15. Gamblin TC, King ME, Dawson H, Vitek MP, Kuret J, Berry RW, Binder LI: In vitro polymerization of tau protein monitored by laser light scattering: method and application to the study of FTDP-17 mutants. Biochemistry 2000, 39:6136–6144
16. Vogelsberg-Ragaglia V, Bruce J, Richter-Landsberg C, Zhang B, Hong M, Trojanowski JQ, Lee VM: Distinct FTDP-17 missense mutations in tau produce tau aggregates and other pathological phenotypes in transfected CHO cells. Mol Biol Cell 2000, 11:4093–4104
17. Alonso AC, Grundke-Iqbal, Iqbal K: Alzheimer's disease hyperphosphorylated tau sequesters normal tau into tangles of filaments and disassembles microtubules. Nat Med 1996, 2:783–787
18. Alonso A, Grundke-Iqbal I, Barra HS, Iqbal K: Abnormal phosphorylation of tau and the mechanism of Alzheimer neurofibrillary degeneration: sequestration of microtubule-associated proteins 1 and 2 and the disassembly of microtubules by the abnormal tau. Proc Nat Acad Sci USA 1997, 94:298–303
19. Connell JW, Gibb GM, Betts JC, Blackstock WP, Gallo J, Lovestone S, Hutton M, Anderton BH: Effects of FTDP-17 mutations on the in vitro phosphorylation of tau by glycogen synthase kinase 3beta identified by mass spectrometry demonstrate certain mutations exert long-range conformational changes. FEBS Lett 2001, 493:40–44
20. Miyasaka T, Morishima-Kawashima M, Ravid R, Heutink P, van Swieten JC, Nagashima K, Ihara Y: Molecular analysis of mutant and wild-type tau deposited in the brain affected by the FTDP-17 R406W mutation. Am J Pathol 2001, 158:373–379
21. Perez M, Lim F, Arrasate M, Avila J: The FTDP-17-linked mutation R406W abolishes the interaction of phosphorylated tau with microtubules. J Neurochem 2000, 74:2583–2589
22. Sahara N, Tomiyama T, Mor HJ: Missense point mutations of tau to segregate with FTDP-17 exhibit site-specific effects on microtubule structure in COS cells: a novel action of R406W mutation. J Neurosci Res 2000, 60:380–387
23. Frappier T, Liang NS, Brown K, Leung CL, Lynch T, Liem RK, Shelanski ML: Abnormal microtubule packing in processes of SF9 cells expressing the FTDP-17 V337M tau mutation. FEBS Lett 1999, 455: 262–266
24. Matsumura N, Yamazaki T, Ihara Y: Stable expression in Chinese hamster ovary cells of mutated tau genes causing frontotemporal dementia and parkinsonism linked to chromosome 17 (FTDP-17). Am J Pathol 1999, 154:1649–1656
25. Perez M, Hernandez F, Gomez-Ramos A, Smith M, Perry G, Avila J: Formation of aberrant phosphotau fibrillar polymers in neural cultured cells. FEBS Lett 2002, 269:1484–1489
26. Dickson DW: Neuropathologic differentiation of progressive supranuclear palsy and corticobasal degeneration. J Neurol 1999, 246:6–15
27. Kenessey A, Nacharaju P, Ko LW, Yen SH: Degradation of tau by lysosomal enzyme cathepsin D: implication for Alzheimer neurofibrillary degeneration. J Neurochem 1997, 69:2026–2038
28. Yen SH, Fields KL: Antibodies to neurofilament glial filament and fibroblast intermediate filament proteins to different cell types of the nervous system. J Cell Biol 1981, 88:115–126
29. Schweers O, Mandelkow EM, Biernat J, Mandelkow E: Oxidation of cysteine-322 in the repeat domain of microtubule-associated protein tau controls the in vitro assembly of paired helical filaments. Proc Natl Acad Sci USA 1995, 92:8463–8467
30. DeTure M, Ko L, Easson C, Hutton M, Yen SH: Inducible expression of wild type tau in H4 neuroglioma cells. Alzheimer's Disease: Advance in Etiology, Pathogenesis and Therapeutics. Edited by K Iqbal, SS Sisodia, B Winblad. New York, John Wiley & Sons Ltd., 2001, pp 6651–6660
31. Ksiezak-Reding H, Liu W-K, Wall JS, Yen SH: Biochemical isolation and characterization of paired helical filaments. Function and Malfunction of the Tau Proteins: Concepts and Approaches. Edited by R Brandt, J Avila, K Kosik. Harwood Academic Publisher, Newark, NJ, 1997, pp 651–660
32. Arawaka S, Usami M, Sahara N, Schellenberg GD, Lee G, Mori H: The tau mutation (val337met) disrupts cytoskeletal networks of microtubules. Neuroreport 1999, 10:993–997
33. Dayanandan R, Van Slegtenhorst M, Mack TG, Ko L, Yen SH, Leroy K, Brion JP, Anderton BH, Hutton M, Lovestone S: Mutations in tau reduce its microtubule binding properties in intact cells and affect its phosphorylation. FEBS Lett 1999, 12:228–232
34. Jicha GA, Berenfeld B, Davies P: Sequence requirements for formation of conformational variants of tau similar to those found in Alzheimer's disease. J Neurosci Res 1999, 55:713–723
35. Daly NL, Hoffmann R, Otvos Jr L, Craik DJ: Role of phosphorylation in the conformation of tau peptides implicated in Alzheimer's disease. Biochemistry 2000, 39:9039–9046
36. Carmel G, Mager EM, Binder LI, Kuret J: The structural basis of monoclonal antibody Alz50's selectivity for Alzheimer's disease pathology. J Biol Chem 1996, 271:32789–32795
37. Jicha GA, Rockwood JM, Berenfeld B, Hutton M, Davies P: Altered conformation of recombinant frontotemporal dementia-17 mutant tau. Neurosci Lett 1996, 260:153–156
38. Hong M, Zhukareva V, Vogelsberg-Ragaglia V, Wszolek Z, Reed L, Miller BI, Geschwind DH, Bird TD, McKeel D, Goate A, Morris JC, Wilhelmsen KC, Schellenberg GD, Trojanowski JQ, Lee VMY: Mutation-specific functional impairments in distinct tau isoforms of hereditary FTDP-17. Science 1998, 282:1914–1917
39. Hasegawa M, Smith MJ, Goedert M: FTDP-17 mutations N279K and S305N in tau produce increased splicing of exon 10. FEBS Lett 1998, 437:207–210
40. DeTure M, Ko L, Yen S, Nacharaju P, Easson C, Lewis J, van Slegtenhorst M, Hutton M, Yen SH: Missense tau mutations identified in FTDP-17 have a small effect on tau-microtubule interactions. Brain Res 2000, 853:5–14
41. Lu M, Kosik KS: Competition for microtubule-binding with dual expression of tau missense and splice isoforms. Mol Biol Cell 2001, 12:171–184